Dalton Transactions

Accepted Manuscript

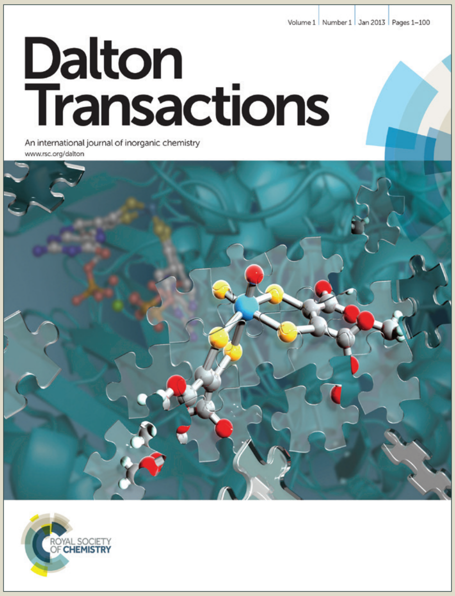

Volume 1 | Number 1 | Jan 2013 | Pages 1–100

Dalton Transactions

An international journal of inorganic chemistry

www.rsc.org/dalton

ROYAL SOCIETY OF CHEMISTRY

ROYAL SOCIETY OF CHEMISTRY

www.rsc.org/dalton

Table of content:

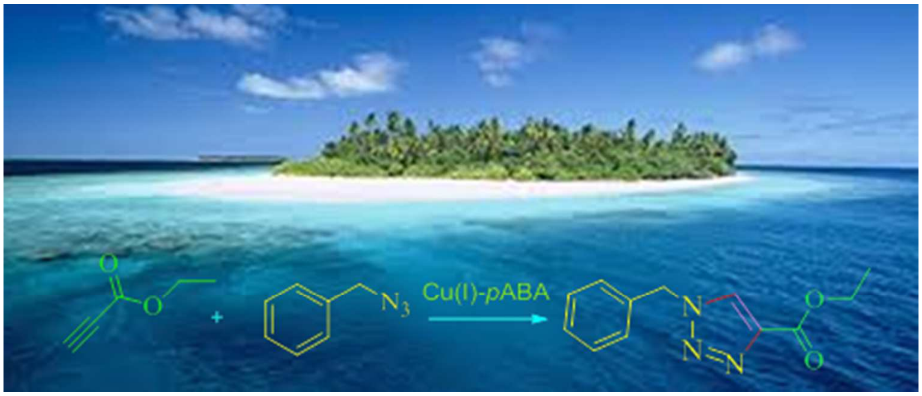

Cu(I)-*polymer* composite recyclable catalyst for the azide-alkyne cycloaddition reaction at room temperature in aqueous medium.

Polymer supported Cu(I) catalyst for 'click reaction' in aqueous media

Rafique Ul Islam,[a] Abu Taher,[a] Meenakshi Choudhary,[a] Michael J Witcomb,[b] Kaushik Mallick [a]*

[a] Department of Chemistry, University of Johannesburg, P.O. Box 524, Auckland Park 2006, South Africa,

[b] DST/NRF Centre of Excellence in Strong Materials, University of the Witwatersrand, Private Bag 3, WITS 2050, South Africa.

* Address correspondence to kaushikm@uj.ac.za

Polymer stabilized monovalent copper has been synthesized using an *in-situ* chemical transformation route and was characterized by means of different microscopic, optical and surface characterization techniques, which offered the information about the chemical structure of polymer and the morphology of the complex. The supramolecular material, Cu(I)–*poly*(2-aminobenzoic acid), Cu(I)-*p*ABA, showed the catalytic activity for the cycloaddition reaction between terminal alkynes and azides to synthesize 1,2,3-triazoles with excellent yields. The catalyst was recovered from the reaction mixture and recycled for several times without appreciable loss of catalytic activity. The whole strategy was done under ambient condition and in presence of water as a solvent.

Keywords: Cu(I)–*poly*(2-aminobenzoic acid), azide-alkyne cycloaddition, click reaction, multicomponent reaction.

Introduction

Catalysis by metal ions is a powerful method of accelerating a large number of organic reactions.[1] An example of a carbon-carbon bond formation reaction is where enantioselective carboalkoxylation of alkynes has been reported catalyzed by gold(I) complexes.[2] Further, a palladium (II) catalyst system, in the presence of 1,2-bis(diphenylphosphino) ethane as the ligand, has been found to be an efficient catalyst for the *N*-alkylation of amines using alcohols under solvent-free conditions.[3] In addition to these, metal ion catalyzed organic transformation reactions utilizing a one-pot process have gained increasing interest as the molecular complexity is rapidly generated without the need for the isolation of intermediates resulting in enhanced efficiency and sustainability.[4-6] Au(I)/Rh(I) dual catalyst system has been reported for the consecutive synthesis of β-disubstituted ketones and asymmetric 1,4-

addition,[7] while poly (3-aminoquinoline) stabilized Pd(I) has been found to act as a catalyst for a Sonogashira cross-coupling reaction for aryl and heteroaryl of iodides and bromides.[8] The participation of metal ions in biological reactions has also been demonstrated. For example, in the presence of O_2, Fe(III) or Cu(II), and an appropriate electron donor, a number of enzymatic and non-enzymatic oxygen free radical-generating systems have been reported to catalyze the oxidative modification of proteins.[9]

Cu(I) catalyzed azide-alkyne cycloaddition (AAC) or Click reaction continues to be of much interest[10] since it offers the opportunity to chemists to connect two potentially complex building blocks under mild conditions.[11] The cycloaddition between an azide and a terminal or internal alkyne to give a 1,4- or 1,5-disubstituted 1,2,3-triazole, was developed by Rolf Huisgen.[12] The lack of regioselectivity and the requirement of high temperature were the major drawbacks of the reaction. The copper(I) catalysts could facilitate the cycloaddition in a regiospecific manner to give only 1,4-disubstituted triazoles and was reported by Sharpless[10] and have attracted significant attention due to their application in the synthesis of pharmaceutical, agrochemical, dye, corrosion inhibitor, biochemical, polymer and other functional materials. This reaction has thus been extensively applied to the synthesis of macromolecules[13] and to the functionalization of biomolecules.[14] AAC reaction has been reported using the catalyst in the form of Cu(I) salt,[15] $CuSO_4$-ascorbate system,[16] immobilized Cu(I) onto polymers[17] or zeolite,[18] copper nanoparticles,[19] metallic copper turnings,[20] nanostructured copper oxide[21] and all of the above copper based catalysts have successfully demonstrated the activity for the title reaction.

The present paper reports on a single-step oxidative polymerization reaction of 2-aminobenzoic acid using copper sulphate as an oxidizing agent, which results in the formation of a Cu(I)-*poly*(2-aminobenzoic acid), Cu(I)-*p*ABA, complex. Special attention has been paid to characterizing the metallo-macromolecule complex by spectroscopic techniques. The as-prepared material showed a high catalytic activity towards azide-alkyne 1,3-dipolar cycloaddition reactions carried out at room temperature, in the presence of water as a solvent, under aerated conditions yielding catalytic efficiency over several cycles. Polymers show the potential benefit as a stabilizer of the catalyst for a wide range of applications.[22-24] The advantage of a polymer as a stabilizer results from its robustness as well as flexibility.[25]

Materials and methods

Materials: Unless otherwise mentioned, all chemicals and reagents used for this study were of analytical grade and were used as received. Ultra-pure water (specific resistivity > 17MΩcm) was used in these experiments.

Synthesis of the Cu(I)–*poly*(2-aminobenzoic acid), Cu(I)-*p*ABA, complex: In a typical experiment, 0.10 g of 2-aminobenzoic acid was dissolved in 25 mL Milli-Q water (60^{o}C) in a beaker. To this, 10 mL of $CuSO_4$, $5H_2O$ solution (10^{-2} mol dm^{-3}, dissolved in dimethylformamide, DMF) was added slowly under continuous stirring conditions. During the addition, the solution took on a green colourization, while at the end; a dark green precipitation was formed at the bottom of the beaker. The entire reaction was performed at room temperature upon open atmosphere condition. The material was allowed to settle for 10 min after which 5 μL of the colloidal solution was taken from the bottom of the conical flask and pipetted onto lacey, carbon-coated, nickel mesh grids for TEM examination. Subsequent to the TEM study, the same grids were sputter coated with a conducting layer a few nanometres thick of Au-Pd and viewed by scanning electron microscopy (SEM). The required amount of material was used for UV-vis and Raman spectroscopy studies. The remaining portion of the compound was dried under vacuum at 60 ^{o}C and used for XRD and XPS measurements as well as for studies of the catalytic properties.

Procedure for the synthesis of phenyl azide, benzyl azide and 2-bromo benzyl azide:
Phenyl azide: Sodium azide (0.78 g, 12 mmol, 1.2 equiv.) and $CuSO_4.5H_2O$ (2.5 g, 10 mmol, 1.0 equiv.) were added in a round bottom flask in presence of methanol (15 mL). To this phenyl boronic acid (1.22 g, 10 mmol, 1.0 equiv.) was added under vigorous stirring conditions at room temperature. The resulting mixture was concentrated under reduced pressure and the residue was extracted with hexane producing a yellow liquid.

Benzyl azide: Benzyl bromide (2.0 mL, 16.84 mmol, 1.0 equiv.) was dissolved in DMSO (40 mL). Sodium azide (1.64 g, 25.26 mmol, 1.5 equiv.) was added as solid and the reaction was stirred overnight at room temperature. Water was added slowly to the reaction mixture and the product was extracted using diethyl ether. The combined diethyl ether layer was washed with brine, dried over anhydrous sodium sulphate and the solvent was removed under reduced pressure to yield benzyl azide.

2-Bromo benzyl azide: 2-Bromo benzyl bromide (2.5 g, 10 mmol, 1.0 equiv.) was dissolved in DMSO (40 mL). Sodium azide (0.975 g, 15 mmol, 1.5 equiv.) was added as solid and the reaction was stirred overnight at room temperature. Water was added slowly to reaction mixture and the product was extracted using diethyl ether. The combined diethyl ether layer was washed with brine, dried over anhydrous sodium sulphate and the solvent was removed under reduced pressure to yield 2-bromobenzyl azide.

General procedure for the cyclo-addition reaction between azide and terminal alkyne: Alkyne (1 equiv.) and azide (1 equiv.) were added in the presence of water (5 mL) in a 25 mL round bottom flask. To this solution, 1 equivalent of triethylamine (TEA) and 10 mg of Cu(I)-*p*ABA catalyst (0.01 mol % of Cu) were added. The reaction mixture was stirred at room temperature for 3-5 h and the reaction was monitored using thin layer chromatography technique. After completion, the reaction mixture was filtered and the residue was washed with methanol. Methanol was evaporated from the filtrate and the latter was extracted using ethyl acetate and subsequently dried over anhydrous sodium sulphate. The combined organic layer was then concentrated under vacuum to give the corresponding triazoles and purified by column chromatography. Compounds were confirmed by comparison with the spectroscopic data described in the relevant literature.

General procedure for the one-pot, multicomponent azide-alkyne cycloaddition: The above mentioned procedure was followed using an alkyl halide **5** (1 equiv.), NaN_3 (1 equiv.) and an alkyne **2** (1 equiv.) in the presence of water (10 mL), triethylamine (1 equiv.) and catalyst (0.01 mol % of Cu) for the cycloaddition reaction in a single pot for 7 h.

Characterization techniques: SEM studies were performed in a FEI FEG Nova 600 Nanolab operating at 2–10 kV. TEM investigations were undertaken at 120 kV in a Philips CM200 TEM equipped with a LaB_6 source. An ultrathin window energy-dispersive X-ray spectrometer and a Gatan Imaging Filter (GIF) attached to the microscope were used to determine the chemical composition of the samples. The UV-vis spectra were recorded using a Shimadzu UV-1800 UV-VIS spectrophotometer with a quartz cuvette. Raman spectra were acquired using the green (514.5 nm) line of an argon ion laser as the excitation source. Light dispersion was undertaken via the single spectrograph stage of a Jobin–Yvon T64000 Raman spectrometer. The X-ray diffraction (XRD) patterns were recorded on a Shimadzu XD-3A X-ray diffractometer operating at 20 kV using Cu-Kα radiation (k = 0.1542 nm). The measurements were performed over a diffraction angle range of $2\theta = 20^o$ to 70^o. The X-ray photoelectron spectra were collected in an ultra-high vacuum chamber attached to a Physical Electronics PHI 560 ESCA/SAM system. Nitrogen adsorption-desorption isotherms were measured with a Quadra-Sorb S1 apparatus at 77 K. The surface areas were calculated by the Brunauer–Emmett–Teller (BET) method, and the pore size distribution was calculated from the desorption branch using the Barett-Joyner-Halenda (BJH) theory. The Thermo Scientifc XSERIES-2 Quadrupole Inductively Coupled Plasma Mass Spectrometer (ICP-MS) instrument was used to calculate the copper concentration due to leaching process. ^{1}H NMR and ^{13}C NMR spectra were recorded on Bruker Ultrashield 400 (400 MHz for ^{1}H and 100 MHz for ^{13}C{^{1}H} in $CDCl_3$).

Results and discussion:

Formation mechanism of the Cu(I)-*p*ABA complex:

The Cu(I)-*p*ABA composite complex was prepared by using an *in-situ* polymerization and composite formation technique[26] in which the formation of the polymer and Cu(I) took place simultaneously. During the addition of copper sulphate to *2*-aminobenzoic acid, the oxidative polymerisation of aminobenzoic acid occurred to form poly-(aminobenzoic acid), *p*ABA, while at the same time, the Cu(II) salts reduced to Cu(I). Further reduction of Cu(I) to Cu(0) nanoparticles was not facilitated probably because the co-ordination of the Cu(I) with the chain nitrogen of the *p*ABA forms an energetically more stable N→Cu(I) type of bond but the exact structure of Cu(I)-*p*ABA has not been established yet. The results of the following characterization techniques support the above statements.

Characterization of the Cu(I)-*p*ABA complex:

Microscopic property: The SEM image (Figure 1A) illustrates the fiber-like morphology of the Cu(I)-*p*ABA complex. A similar morphology was obtained when the ratio of copper sulphate to 2-aminobenzoic acid was altered. Various sizes and dimensions of the fibers were seen within the branch of the polymer. Focusing the high intensity electron beam on the sample was not able to distort the structure suggesting a high level of rigidity of the polymer. The TEM image (Figures 1B) shows the internal microstructure of the polymer. It should be noted that further reduction of Cu(I) species to Cu(0) is possible during TEM observations if the sample is exposed to the electron beam for an extended period or when the beam is focussed onto a given area. The viewing conditions were chosen here such that this reduction did not occur. The surface of the samples was found to be smooth while there was no evidence of the presence of copper nanoparticles within or on the polymer. To confirm this, X-ray diffraction (XRD) and X-ray photoelectron spectroscopy (XPS) measurements were undertaken. Energy-dispersive X-ray (EDX) spectra was obtained from the electron beam being focused onto the Cu(I)-*p*ABA sample and yielded copper X-ray peaks situated at the binding energies of 0.85, 8.05, and 8.95 keV belong to CuL$_1$, CuK$_\alpha$, and CuK$_\beta$, respectively. The representative EDX Spectra for Cu(I)-*p*ABA sample is available in Electronic Supplementary Information Fig. S1 (ESI). The Ni peak is derived from the TEM support grid.

Surface analysis: The XRD pattern of polyaniline and the derivatives generally varies as a consequence of the nature of the synthesis route, solvent utilized for the synthesis, the oxidation state and the chain length of the polymer.[27] In the present study, the XRD pattern of Cu(I)-*p*ABA (Figure 2A) confirmed the crystalline character of the *poly* (2-aminobenzoic acid), and showing no indication of the formation of metallic copper. The XRD pattern of *p*ABA is available in Electronic Supplementary Information Fig S2 (ESI). The XPS spectrum (Figure 2B) shows a single Cu 2p$_{3/2}$ peak at 933.40 eV, which suggests the presence of Cu(I) in the sample.[28] XPS analysis also confirmed that 1.06 wt% Cu was present on the surface of the polymer matrix.

Optical characterization: The UV-vis spectrum of Cu(I)-*p*ABA complex is shown in Figure 3A. A shoulder-like appearance at 330 nm corresponds to the π–π* transition of the benzenoid rings, an inter-band transition. Again, in the present study, within the range between 400–700 nm, the resultant complex material showed a broad absorption spectra with an absorption peak at 500 nm and this behaviour might be due to the combined effect of (a) polaron–bipolaron transition, that shows the absorption band within the range of 400–440 nm and (b) benzenoid to quinoid excitonic transition.[29,30] The position of the excitonic peak is sensitive to the nature of the counter-ions, the solvent and to the chemical structure of the polymer.[31]

Figure 3B shows a typical Raman spectrum recorded from the Cu(I)-*p*ABA supramolecular material. In the 1700 and 1000 cm^{-1} range the bands derived from Raman spectra involve the poly-(aminobenzoic acid) oxidation state. The spectrum of polymer reveals C–C stretching deformation bands of benzene ring at 1602 and 1575 cm^{-1}, which are characteristic of the semiquinone structure.[32,33] Another peak appeared at 1500 cm^{-1} corresponds to the N–H bending deformation band as a result of the interaction of the Cu(I) with nitrogen. Three prominent peaks at 1390, 1427 and 1450 cm^{-1} correspond to the C–N$^{\bullet+}$ stretching modes, the intensity of the peak at 1390 cm^{-1} confirming the high concentration of these species present in the polymer. The bands between 1200–1300 cm^{-1} can be assigned to C–N stretching modes. The position of the benzene C–H bending deformation band at 1175 cm^{-1} is again characteristic of the reduced and semiquinone structures. The above mentioned bands indicate the presence of both quinoid and benzenoid structures in poly-(aminobenzoic acid).

Gas adsorption property: According to Figure 4, the nitrogen adsorption and desorption isotherms of Cu(I)-*p*ABA possess a type II isotherm with a typical H3-type hysteresis loop according to the IUPAC (International Union of Pure and Applied Chemistry) classification. The corresponding pore size distribution curve by the Barrett-Joyner-Halenda (BJH) method demonstrates that the pore diameters are in the range from 25 to 35 nm (inset, Figure 4). The BET surface area of the sample was calculated to be 7.8 $m^2.g^{-1}$.

Catalytic property of the Cu(I)-*p*ABA supramolecular composite: The Cu(I)-*p*ABA composite material was used as an catalyst for 1,3-dipoar cycloaddition for the synthesis of di-substituted 1,2,3-triazoles using benzyl azide, **1a**, with phenyl acetylene, **2a**, at room temperature in the presence triethyl amine (Et_3N) under different solvent conditions such as dichloromethane, chloroform, toluene, ethanol, methanol and water (Table 1). Before that the thermal stability of the catalyst was measured using differential scanning calorimetry (DSC) technique. The DSC thermogram shows the superior thermal stability of the Cu(I)-*p*ABA in comparison with pure polymer (*p*ABA). Details DSC study is available in Electronic Supplementary Information Fig S3 (ESI). In the absence of Cu(I)-*p*ABA, there was no sign of the formation of the product 1-benzyl-4-phenyl-1*H*-1,2,3-triazole **(3a)** (entry 1). Using Cu(I)-*p*ABA as a catalyst, the desired coupled product has been achieved with varying yields (entries 2-6) in presence of different solvents (dichloromethane, chloroform, toluene, ethanol, methanol and water). The combination of methanol, methanol-water (1:1) and water alone (entries 3-5) gave the highest product conversion among all the solvents tested in Table 1. Further optimization of the reaction was performed by varying the catalyst loading. The best result was achieved when the catalyst concentration was 0.01 mol% of Cu in methanol / methanol-water (1:1) / water used as a solvent (Table 1, entries 3–5). Increasing the amount of catalyst concentration by a factor of 10, no further improvement in the product yield was recorded (Table 1, entry 6). Further to the above, the reaction between benzyl azide with phenyl acetylene was also carried out in the absence of Et_3N and in the presence of the catalyst (Cu(I)-*p*ABA) to determine the significance of Et_3N in the reaction. We observed that the most appropriate reaction conditions in which our catalyst performed efficiently was in the environment of $Et_3N–H_2O$. The product, 1-benzyl-4-phenyl-1*H*-1,2,3-triazole **(3a)**, was characterised by spectroscopic methods and found to be identical with that reported one.[34] As a consequence of the above results, by considering both an economic and an environmental aspect, it was decided to use only water as a solvent for the rest of the study.

Based on the above optimized reaction conditions, we explored the versatility of the catalyst for the 1,3-dipolar cycloaddition of structurally diverse azides and alkynes, and the results are summarized in Tables 2 and 3. All the substrates produced the expected cycloaddition product with very good to excellent yields and selectivity.

It was found that a yield of 98% of the cycloaddition product, 1-benzyl-4-phenyl-1*H*-1,2,3-triazole, has been obtained for the coupling between benzyl azide and phenylacetylene (Table 2, entry 1). The coupling of phenyl azide with phenylacetylene (Table 2, entry 6) resulted the product, 1, 4-diphenyl-1*H*-1,2,3-triazole, with the yield of 97%. To achieve a comparable yield value for the coupling product between benzyl azide with phenylacetylene and phenyl azide with phenylacetylene, a longer reaction time was required for the later and that can be explained in terms of an adjacent steric crowding effect due to the presence of benzene ring. The coupling between ethyl propiolate with benzyl and phenyl azide (Table 2, entries 2 and 7) produced 90% of the products (ethyl 1-benzyl-1*H*-1,2,3-triazole-4-carboxylate, **3b,** and ethyl 1-phenyl-1*H*-1,2,3-triazole-4-carboxylate, **3g**) has been obtained within 3 and 5 hours of reaction duration respectively. The structure of the compound **3g** has been identified by the single crystal X-ray crystallography[35] as shown in Figure 5. When prop-2-*yn*-1-ol was coupled with benzyl azide (Table 2, entry 3), a decrease in yield (84%) has been observed of the cycloaddition product. Coupling between 1-ethynyl-4-(trifluoromethoxy) benzene and benzyl azide produced the cycloaddition product, 1-benzyl-4-(4-(trifluoromethoxy)phenyl)-1*H*-1,2,3-triazole, with a yield of 86% (Table 2, entry 4). The presence of electron donating group in the alkynes does not have much effect towards the yield of cycloaddition product. Cycloaddition reaction between 1-ethynyl-4-methoxybenzene with both benzyl and phenyl azide produced 87 and 86% yield, respectively (Table 2, entries 5 and 8) within 3 and 5 hours of reaction duration respectively. The coupling between phenyl acetylene and 1-azido-4-methoxybenzene produced the cycloaddition product, 1-(4-methoxyphenyl)-4-phenyl-1*H*-1,2,3-triazole, with a yield of 95% (Table 2, entry 9). Almost identical amount of cycloaddition product, 1-(naphthalen-1-yl)-4-phenyl-1*H*-1,2,3-triazole, has been obtained when phenyl acetylene reacted with 1-azidonaphthalene, (Table 2, entry 10), within 5h of reaction duration. The cycloaddition of 2-bromobenzyl azides with different alkynes (Table 3, entries 1-5) shows an identical reactivity trend to that found for the benzyl azide (Table 2, entries 1-5).

The recyclability of the catalyst: After identified water as the suitable solvent for the above reactions, we investigated the scaling up of the title reaction and the recyclability of the Cu(I)-*p*ABA catalyst using benzyl azide and phenylacetylene as reactants. We increased ten fold the amount of both the catalyst and the reactants, and performed the experiment under the previous reaction conditions. After the first run, the product was extracted with ethyl acetate and the residual catalyst was reused four times under the same conditions. The results indicated that the used material was also active as a catalyst without a significant loss of catalytic performance (Figure 6A). At the end of the fifth cycle, a yield of 83% of the coupled product has been achieved. The catalyst was characterized by TEM at the conclusion of the first cycle. The presence of the copper nanoparticles was clearly noted (dark spots with wide size distribution, 10–40 nm, Figure 6B, some of them are circled). In the case of nanoparticles, the surface of the particles is considered to be more reactive as a catalyst as the surface area to volume ratio of the catalyst particles increases significantly as its size decreases to the nano level. In the present scenario, the results of the catalytic activity studies during the recycling process did not show any noticeable effect of nanoparticles in terms of yield or time for the completion of the reaction, which implies that both Cu(I) and the copper nanoparticle species were almost equally active as a catalyst for cycloaddition reaction. It is also important to mention that ICP-MS (inductively coupled plasma mass spectrometry) analysis did not provide any indication for the leaching of copper species at any stage of the recyclability study of the catalyst. The gradual decrease of the yield with recycling was mainly due to the loss of catalyst species during the washing process. For each subsequent cycle, the fresh reaction mixture had a lower amount of copper present in the catalyst which affected the yield.

Cycloaddition reaction using a one-pot multicomponent system: For many organic transformations, the reaction sequences are not as efficient as enzymatic reactions in terms of selectivity and also from an economic point of view. The ideal reaction strategy for the preparation of structurally complex substances would involve sequences in which stereo-controlled formation of bonds occur in a single step starting from simple, readily available materials. As a result, great attention has been given to the development of multicomponent reactions. In the present work, we also directed our attention towards the one-pot, three-component Click reaction (Table 4) in which the azide-alkyne cycloaddition products were generated *in-situ* from their precursor, aryl bromides, sodium azide and alkyne, by deleting one step. The Cu(I)-*p*ABA catalyst again performed well as a catalyst in water in the presence of triethyl amine to give the desired products (Table 4, entries 1–10) in good to excellent isolated yields ranging from 85-94% with a longer period of reaction time (7 hours) to complete.

Kinetic study of the cycloaddition reaction: The kinetic study of the title reaction, in the presence of a Cu(I)-*p*ABA catalyst (0.01 mol% Cu) at room temperature (25 ^{o}C) using H_2O as a solvent for the period of seven hours, has been performed for (a) benzyl azide with phenyl acetylene in the presence of triethyl amine, (b) benzyl azide with phenyl acetylene in the absence of triethyl amine and (c) for the three component system, benzyl bromide, sodium azide and phenyl acetylene in the presence of triethyl amine (Figure 7). From this graph, it is clear that a higher conversion was achieved when triethyl amine was used as a base for both (a) and (c). For (a), about 97% cycloaddition product was recorded in 180 min whereas only a 55% cycloaddition product was obtained within the same time period for (b). For (b), the rate of the reaction was retarded due to the absence of the base. For the reaction with the multicomponent system (curve c), a steady conversion of the reactants was observed resulting in around 93% of cycloaddition product in 390 min. No further increase in conversion was indicated after an additional 30 mins. From Figure 7, curve b, it is clear that in the absence of the base, the induction time of the reaction was longer so there was no indication of product formation in the first 30 min whereas in (a) and (c) no such induction period was observed when triethyl amine was used in the reaction. In absence of a base 76% of cycloaddition product has been achieved clearly indicates the importance of base for a Click reaction to obtain a higher yield.

The most accepted mechanistic pathway for the Cu(I)-*p*ABA catalysed cycloaddition reaction is illustrated in Scheme 1. Since Cu(I) is considered to be the most active species for this reaction, the mechanism thus involves the formation of a Cu(I)-acetylidine complex through the coordination with alkyne followed by the addition with the azide group to give 1,2,3-triazole. It is worth to mention that, under the standard reaction conditions, all the reactions were highly regioselective towards 1,4-disubstituted triazoles. Simple workup operations involving filtration, solvent evaporation and/or column chromatography techniques were applied, furnishing the corresponding 1,2,3-triazoles with excellent isolated yields and selectivity irrespective of nature of the substrates.

Conclusions:

In summary, the present study illustrates the feasibility and the applicability of utilizing a Cu(I)-*p*ABA composite material, synthesized from the precursors of Cu(II) sulphate and (*2*-aminobenzoic acid), to catalyse azide-alkyne cycloaddition at room temperature in the presence of water. The process is environment friendly and uses an easily available solvent to produce excellent yields. Moreover, the execution of the reaction was performed easily using a one-pot, multicomponent strategy to provide the target 1,2,3-triazoles with excellent yields and selectivity. The recyclability of the catalyst without the loss of significant efficiency together with the scope for the scaling up of the reaction indicates the potential of the material as an efficient catalyst.

Acknowledgement:

The authors (RUI, AT, MC and KM) acknowledge financial support from the Research Committee and the Faculty of Science of the University of Johannesburg. MJW gratefully thanks the National Research Foundation (NRF), South Africa for financial support.

References:

1 M. L. Bender, Metal Ion Catalysis of Nucleophilic Organic Reactions in Solution. In *Reactions of Coordinated Ligands and Homogeneous Catalysis*; Busch, D.H., Ed.; American Chemical Society: Washington, USA, 1962, pp. 19-36.

2 W. Zi and F. D. Toste, *J. Am. Chem. Soc.,* 2013, **135**, 12600-12603.

3 T. T. Dang, B. Ramalingam, S. P. Shan and A. M. Seayad, *ACS Catal*., 2013, **3**, 2536-2540.

4 D. J. Arriola, E. M. Carnahan, P. D. Hustad, R. L. Kuhlman and T. T. Wenzel, *Science*, 2006, **312**, 714-719.

5 N. Jeong, S. D. Seo and J. Y. Shin, *J. Am. Chem. Soc*., 2000, **122**, 10220-10221.

6 B. Zimmermann, J. Herwig and M. Beller, *Angew. Chem., Int. Ed*., 1999, **38**, 2372-2375.

7 M. M. Hansmann, A. S. K. Hashmi and M. Lautens, *Org. Lett*., 2013, **15**, 3226-3229.

8 R. Islam, S. K. Mahato, S. K. Shukla, M. J. Witcomb and K. Mallick, *ChemCatChem*, 2013, **5**, 2453-2461.

9 E. R. Stadtman, *Free Radic. Biol. Med*., 1990, **9**, 315-325.

10 V. V. Rostovtsev, L. G. Green, V. V. Fokin and K. B. Sharpless, *Angew. Chem., Int. Ed.*, 2002, **41**, 2596-2599.

11 V. D. Bock, H. Hiemstra and J. H. van Maarseveen, *Eur. J. Org. Chem.*, 2006, **1**, 51-68.

12 R. Huisgen, in 1,3-Dipolar Cycloaddition Chemistry, ed. A. Padwa, Wiley, New York, 1984.

13 G. Franc and A.K. Kakkar, *Chem. Soc. Rev.*, 2010, **39**, 1536-1544.

14 P. M. Gramlich, C. T. Wirges, A. Manetto and T. Carell, *Angew. Chem., Int. Ed.*, 2008, **47**, 8350-8358.

15 C. W. Tornøe, C. Christensen and M. Meldal, *J. Org. Chem.*, 2002, **67**, 3057-3064.

16 V. O. Rodionov, S. I. Presolski, S. Gardinier, Y.-H. Lim and M. G. Finn, *J. Am. Chem. Soc.*, 2007, **129**, 12696-12704.

17 (a) C. Girard, E. Önen, M. Aufort, S. Beauvière, E. Samson and J. Herscovici, *Org. Lett.*, 2006, **8**, 1689-1692. (b) S.-Q. Bai, L. L. Koh and T. S. Andy Hor, *Inorg. Chem.,* 2009, **48**, 1207-1213; (c) S.-Q. Bai, L. Jiang, J.-L. Zuo and T. S. Andy Hor, *Dalton Trans.,* 2013, **42**, 11319–11326; (d) L. Jiang, Z. Wang, S.-Q. Bai and T. S. Andy Hor, *Dalton Trans.,* 2013, **42**, 9437–9443.

18 S. Chassaing, M. Kumarraja, A. S. S. Sido, P. Pale and J. Sommer, *Org. Lett.*, 2007, **9**, 883-886.

19 G. Molteni, C. L. Bianchi, G. Marinoni, N. Santo and A. Ponti, *New J. Chem.*, 2006, **30**, 1137-1139.

20 F. Himo, T. Lovell, R. Hilgraf, V. V. Rostovtsev, L. Noodleman, K. B. Sharpless and V. V. Fokin, *J. Am. Chem. Soc.*, 2005, **127**, 210-216.

21 J. Y. Kim, J. C. Park, H. Kang, H. Song and K. H. Park, *Chem. Commun.*, 2010, **46**, 439-441.

22 E. Granot, E. Katz, B. Basnar and I. Willner, *Chem. Mater.*, 2005, **17**, 4600-4609.

23 X. Feng, C. Mao, G. Yang, W. Hou and J.-J. Zhu, *Langmuir*, 2006, **22**, 4384-4389.

24 R. J. Tseng, J. Huang, J. Ouyang, R. B. Kaner and Y. Yang, *Nano Lett.*, 2005, **5**, 1077.

25 H. Dong, M. Zhu, J. A. Yoon, H. Gao, R. Jin and K. Matyjaszewski, *J. Am. Chem. Soc.*, 2008, **130**, 12852-12853.

26 (a) K. Mallick, M. J. Witcomb, A. Dinsmore and M. S. Scurrell, *Macromol. Rapid Commun.*, 2005, **26**, 232-235; (b) K. Mallick, M. J. Witcomb and M. S. Scurrell, *Eur. Phys. J. E.*, 2006, **19**, 149-154; (c) K. Mallick, M. J. Witcomb, A. Dinsmore and M. S. Scurrell *Langmuir*, 2005, **21**, 7964-7967; (d) K. Mallick, M. J. Witcomb, R. Erasmus and A. Strydom, *J. Appl. Phys.,* 2009, **106**, 074303; (e) K. Mallick, M. J. Witcomb and M. S.

Scurrell, *Eur. Phys. J. E.*, 2006, **20**, 347-353; (f) K. Mallick, M. J. Witcomb and M. S. Scurrell, J. Macromol. *Sci. Pure Appl. Chem.*, 2006, **43**, 1469-1476; (g) S. Scalzullo, K. Mondal, M. J. Witcomb, A. Deshmukh, M. Scurrell and K. Mallick, *Nanotechnology*, 2008, **19**, 075708; (h) K. Mallick, M. J. Witcomb, M. S. Scurrell and A. Strydom, *J. Phys. D: Appl. Phys.*, 2009, **42**, 095409; (i) K. Mallick, M. J. Witcomb and M. S. Scurrell, *J. Phys. Condens. Matter*, 2007, **19**, 196225.

27 Y. Li, X. Zhao, Q. Xu, Q. Zhang and D. Chen, *Langmuir*, 2011, **27**, 6458-6463.

28 W. L. Ong, H. Huang, J. Xiao, K. Zeng and G. W. Ho, *Nanoscale*, 2014, **6**, 1680-1690.

29 K. Mallick, M. Witcomb, M. Scurrell and A. Strydom, *Chem. Phys. Lett.*, 2010, **494**, 232–236.

30 G. Louarn**,** M. Lapkowski, S. Quillard, A. Pron, J. Buisson and S. Lefrant, *J. Phys. Chem.*, 1996, **100**, 6998-7006.

31 J. Stejskal, M. Trchová, J. Prokeš and I. Sapurina, *Chem. Mater.*, 2001, **13**, 4083-4086.

32 M. Tagowska, B. Palys and K. Jackowska, *Synth. Met.*, 2004, **142**, 223-229.

33 M. Łapkowski, K. Berrada, S. Quillard, G. Louarn, S. Lefrant and A. Pron, *Macromolecules*, 1995, **28**, 1233-1238.

34 F. Alonso, Y. Moglie, G. Radivoy and M. Yus, *Tetrahedron Lett.*, 2009, **50**, 2358-2362.

35 CCDC 984755 contains the supplementary crystallographic data for the compound **3g**. These data can be obtained free of charge from The Cambridge Crystallographic Data Centre via www.ccdc.cam.ac.uk/data_request/cif.

Figure Captions:

Figure: 1

Representative (A) SEM and (B) TEM image of the Cu(I)-*p*ABA complex. No evidence of the formation of copper nanoparticles was seen from the TEM image.

Figure: 2

XRD pattern (A) indicates the crystalline character of the polymer and no indication of the presence of metallic copper. The XPS analysis (B) shows a single Cu $2p_{3/2}$ peak at 933.40 eV that corresponds to the presence of Cu(I) species in the sample.

Figure: 3

The UV-vis spectrum (A) of the Cu(I)-*p*ABA complex with a shoulder-like appearance at 330 nm corresponds to the π–π^* transition of the benzenoid rings whereas the polaron/bipolaron transition is positioned at about 400 nm. In the Raman spectrum (B) two high intensity peaks at 1602 and 1575 cm^{-1} reveal the C–C deformation bands of benzenoid unit whereas the benzene C–H bending deformation band at 1175 cm^{-1} indicates the presence of quinoid rings.

Figure: 4

Nitrogen adsorption and desorption isotherms and pore size distribution of the Cu(I)-*p*ABA composite (in-set).

Figure: 5

ORTEP diagram of compound **3g**.

Figure: 6

(A) The histogram from the recyclability study of the Cu(I)-*p*ABA catalytic system shows that the used material was active as a catalyst without a significant loss of catalytic performance. At the end of the fifth cycle, a yield of 83% of the coupled product was achieved. (B) The TEM image of the used catalyst at the end of the first cycle reveals the formation of copper nanoparticles (some of them are indicated within circles) with a wide range of size distribution, 10–40 nm.

Figure: 7

Kinetic study of the azides and alkynes cyclo-addition reactions for (a) benzyl azide with phenyl acetylene in the presence triethyl amine, (b) benzyl azide with phenyl acetylene in the absence of triethyl amine and (c) three-component system, benzyl bromide, sodium azide and phenyl acetylene in the presence triethyl amine using the Cu(I)-*p*ABA catalyst (0.01 mol% of Cu) at room temperature for a period of 7 hours.

Scheme caption:

Scheme: 1

Proposed mechanism of the azide-alkyne cycloaddition reaction.

Figure: 1

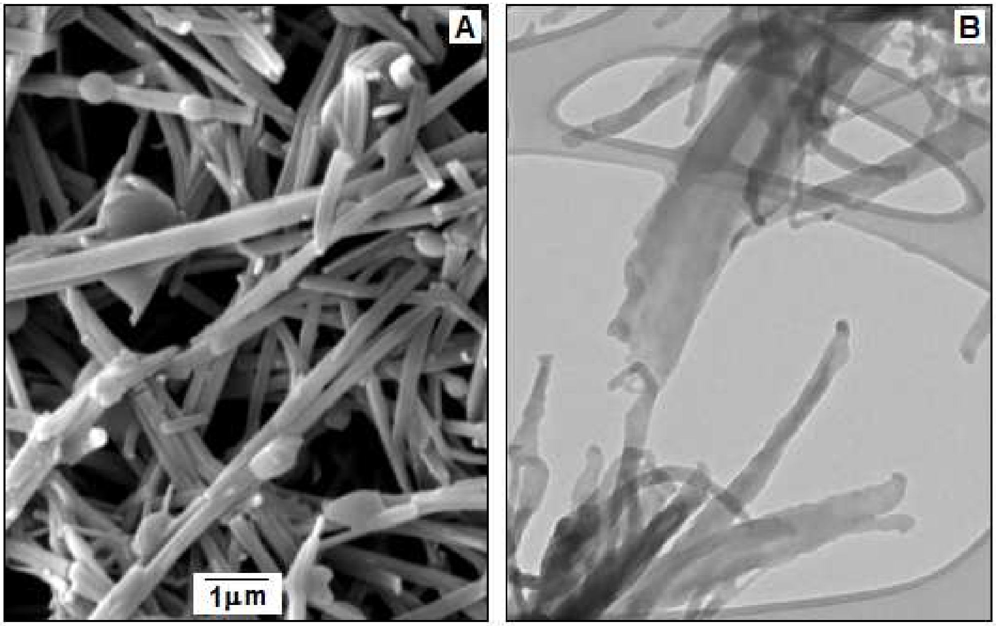

Figure: 2

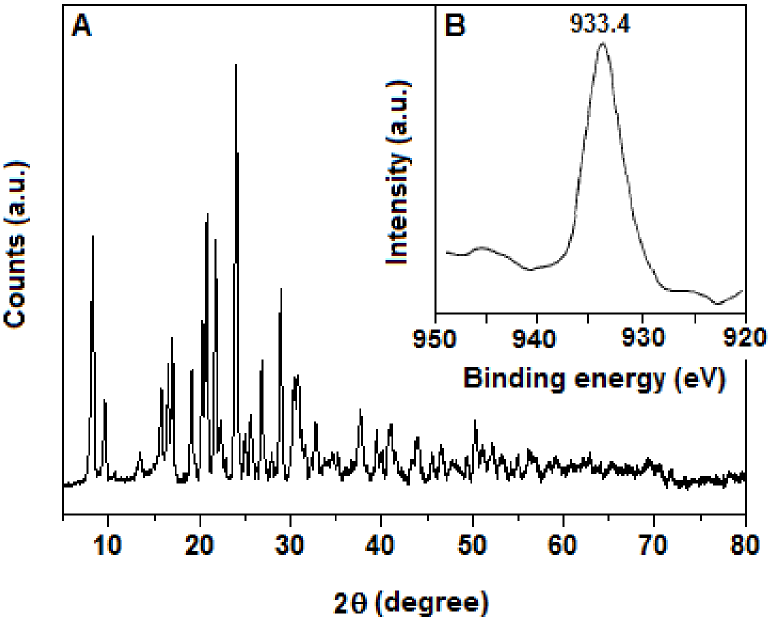

Figure: 3

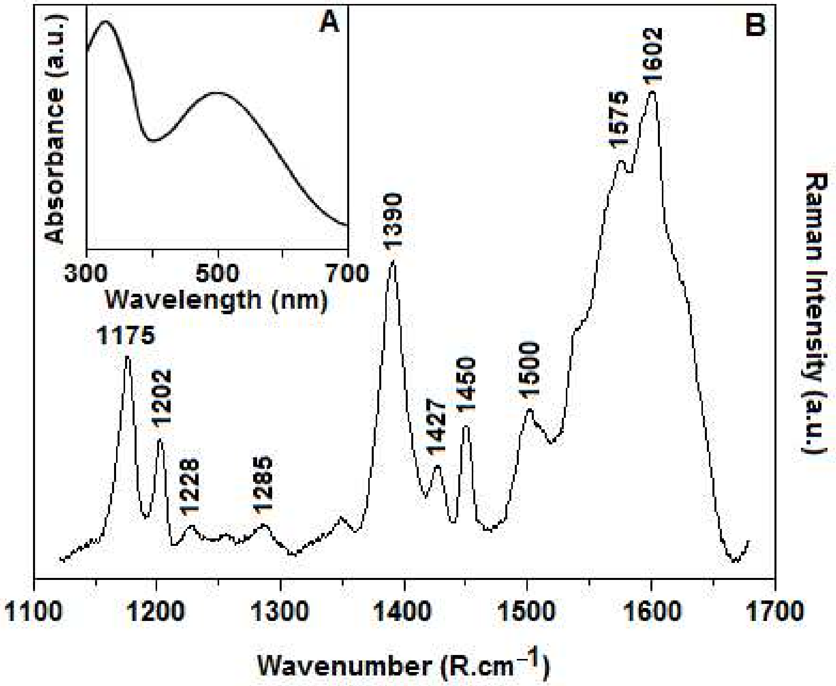

Figure: 4

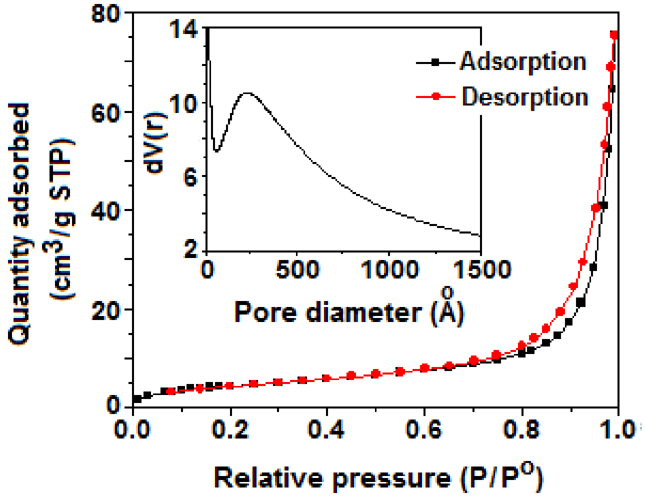

Figure: 5

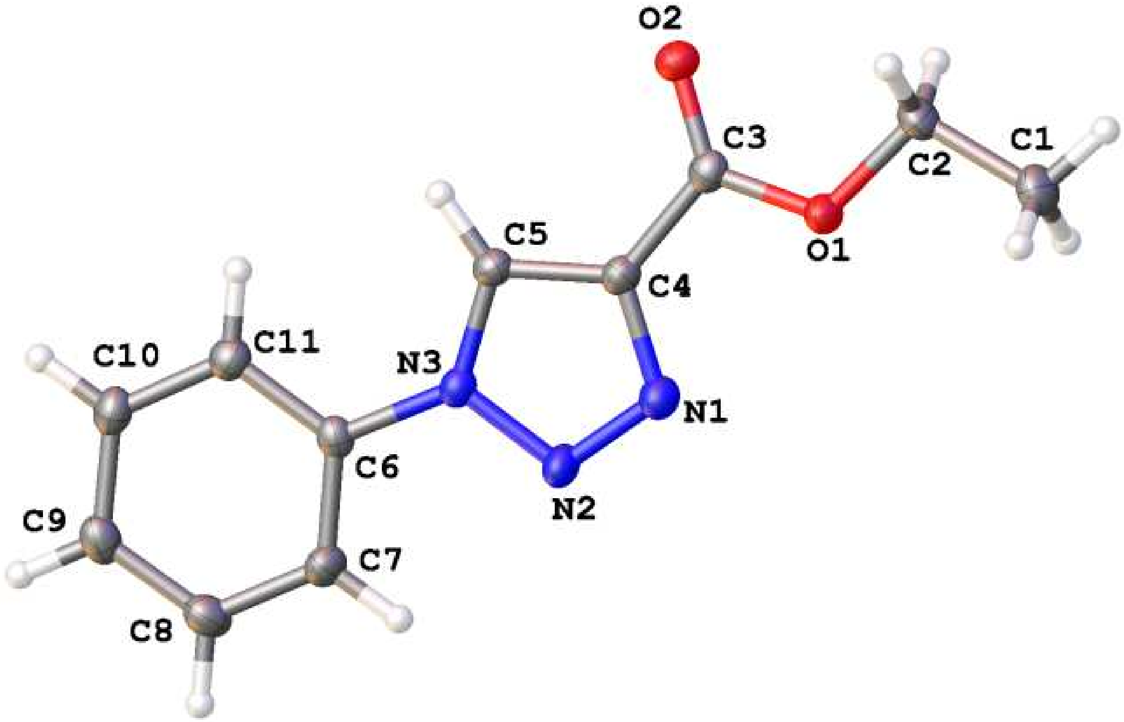

Figure: 6

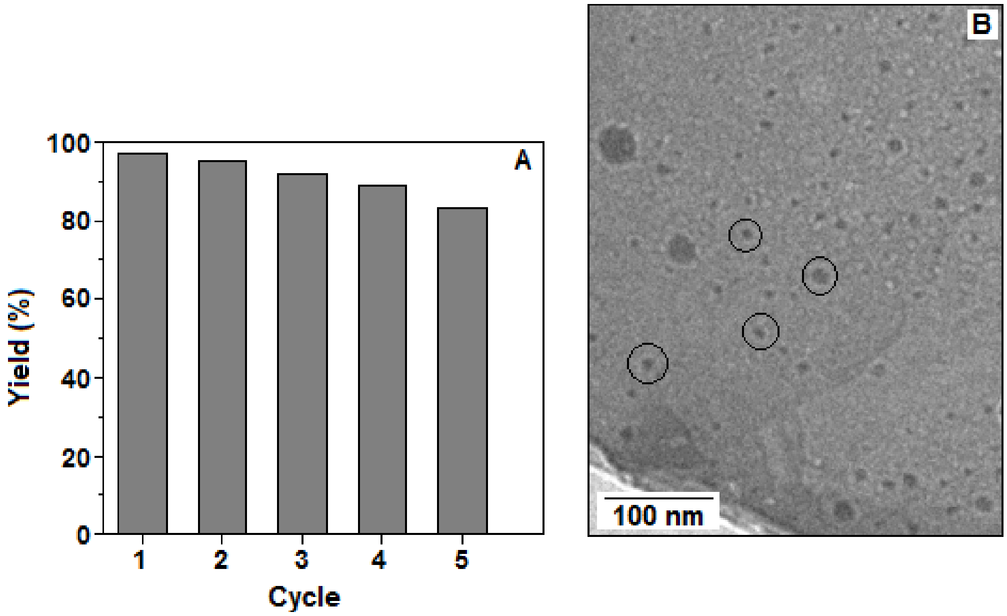

Figure: 7

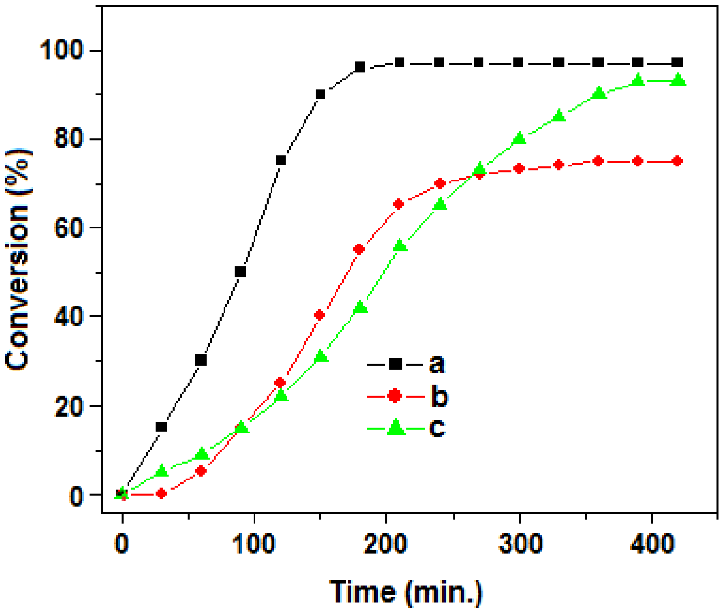

Scheme: 1

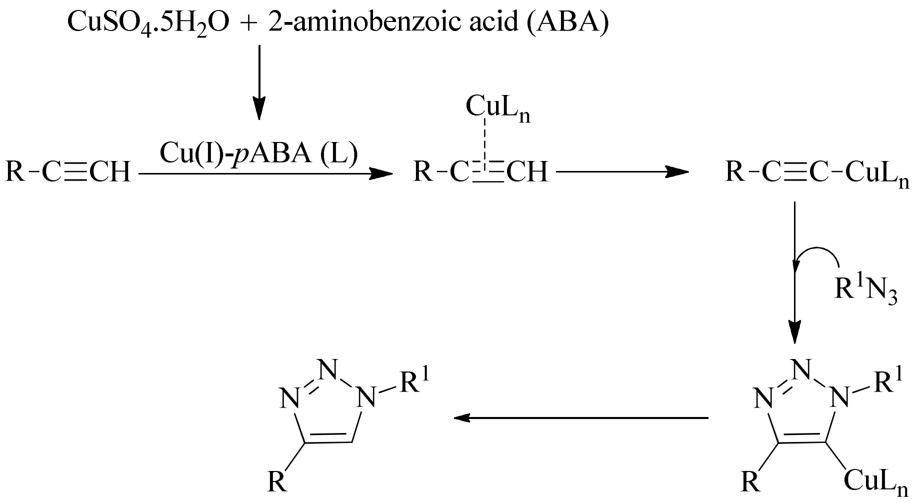
CuSO4.5H2O + 2-aminobenzoic acid (ABA)
R-C≡CH
Cu(I)-pABA (L)
CuLn
R-C≡CH
R-C≡C-CuLn
R1N3
N
N
N
R1
R
CuLn

Table 1: Solvent and catalyst optimization Studies.[a]

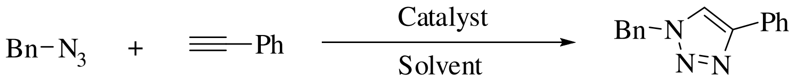

1a **2a** **3a**

Entry	Catalyst conc. (mol% of Cu)	Solvent	Time (h)	Yield(%)
1	Cu-*p*ABA (0.0)	DCM/ $CHCl_3$/ Toluene/ EtOH/ MeOH/ H_2O	24	-
2	Cu-*p*ABA (0.01)	DCM/ $CHCl_3$/ Toluene/ EtOH	3-5	81-86
3	Cu-*p*ABA (0.01)	MeOH	3	97
4	Cu-*p*ABA (0.01)	MeOH : H_2O (1:1)	3	97
5	**Cu-*p*ABA (0.01)**	**H_2O**	**3**	**97**
6	Cu-*p*ABA (0.1)	MeOH/ MeOH:H_2O/ H_2O	3	97

[a] Reaction conditions: **1a** (1.0 mmol), **2a** (1.0 mmol) and triethyl amine (1.0 mmol) at room temperature.

Table 2: Cu(I)-*p*ABA catalyzed azide-alkyne cycloaddition of benzyl and phenyl azides with different alkynes.[a]

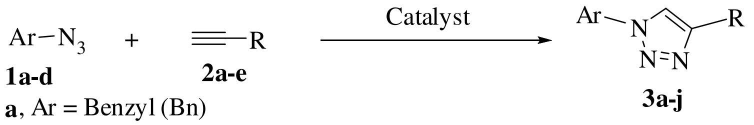

1a-d **2a-e** **3a-j**

a, Ar = Benzyl (Bn)
b, Ar = Phenyl (Ph)
c, Ar = 4-OMePh (Ar')
d, Ar = 1-Naphthyl (Nap)

Entry	Azides (**1**)	Alkynes (**2**)	Products (**3**)[b,c]	Yields (%)
1	**a**	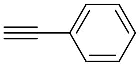 **a**	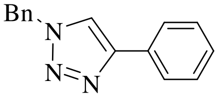 **a**	98
2	**a**	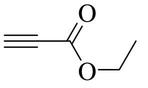 **b**	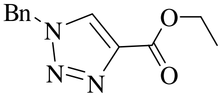 **b**	90
3	**a**	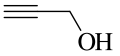 **c**	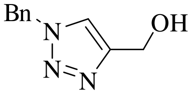 **c**	84
4	**a**	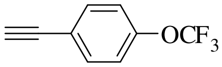 **d**	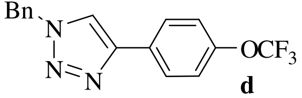 **d**	86
5	**a**	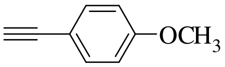 **e**	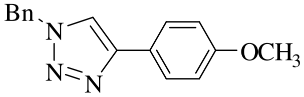 **e**	87
6	**b**	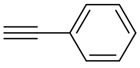 **a**	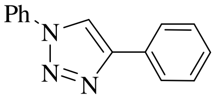 **f**	97
7	**b**	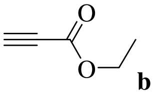 **b**	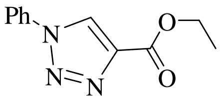 **g**	90
8	**b**	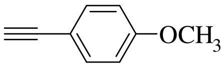 **e**	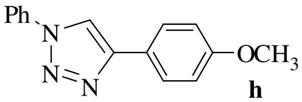 **h**	86
9	**c**	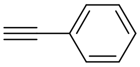 **a**	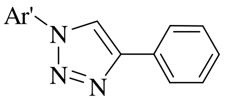 **i**	95
10	**d**	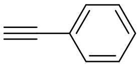 **a**	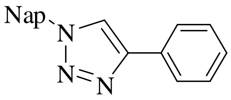 **j**	91

[a] All reactions were carried out in water in the presence of the Cu(I)-*p*ABA catalyst (0.01 mol% Cu) and triethyl amine base (1 equiv.) at room temperature.

[b] Reactions with benzyl azides (**1a**) were under taken for 3 h.

[c] Reactions with aryl azides (**1b, 1c, 1d**) were under taken for 5 h.

Table 3: Cu(I)-*p*ABA catalyzed azide-alkyne cycloaddition of 2-bromobenzyl azides with different alkynes[a]

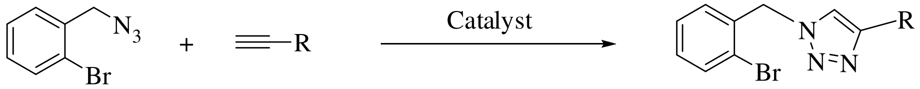

1c **2a-e** **4a-e**

Entry	Alkynes (**2**)	Products (**4**)	Yields (%)
1	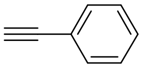 **a**	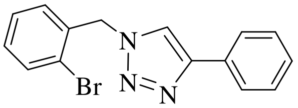 **a**	98
2	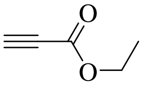 **b**	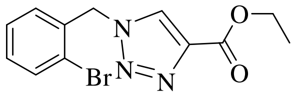 **b**	91
3	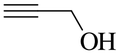 **c**	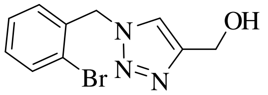 **c**	90
4	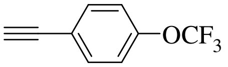 **d**	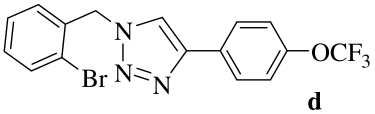 **d**	90
5	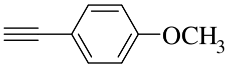 **e**	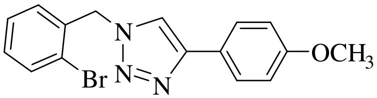 **e**	88

[a] All reactions were carried out in water in the presence of the Cu(I)-*p*ABA catalyst (0.01 mol% Cu) and triethyl amine base (1 equiv.) at room temperature for 3 h.

Table 4: Azide-alkyne cycloaddition using a polymer composite catalyst.[a]

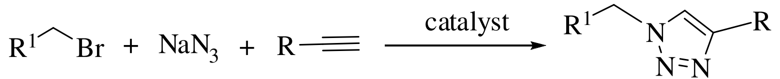

5 a,b **2a-e** **3a-e, 4a-e**

a, R^1 = Ph

b, R^1 = *o*-BrPh

Entry	Products (**3**,**4**)	Yields (%)[b]
1	**3a**	93
2	**3b**	90
3	**3c**	86
4	**3d**	90
5	**3e**	87
6	**4a**	94
7	**4b**	93
8	**4c**	92
9	**4d**	88
10	**4e**	85

[a] Alkyl halide **5** (1 equiv.), NaN_3(1 equiv.), alkyne **2** (1 equiv.) and Cu(I)-*p*ABA catalyst (0.01 mol% Cu), triethyl amine (1 equiv) at room temperature.

[b] All reactions were caried out over a period of 7 h.